POLITECNICO DI TORINO
Repository ISTITUZIONALE

Altitudinal dependence of projected changes in occurrence of extreme events in the Great Alpine Region

(Article begins on next page)

19 April 2024

RESEARCH ARTICLE

International Journal of Climatology

RMetS

Altitudinal dependence of projected changes in occurrence of extreme events in the Great Alpine Region

Anna Napoli[1,2,3,4] 🄳 | **Antonio Parodi**[1] | **Jost von Hardenberg**[5,6] |
Claudia Pasquero[6,7]

[1]CIMA Research Foundation, Savona, Italy

[2]Department of Computer Science, Bioengineering, Robotics and Systems Engineering, University of Genova, Genoa, Italy

[3]Department of Civil, Environmental and Mechanical Engineering, University of Trento, Trento, Italy

[4]Center Agriculture Food Environment (C3A), Trento, Italy

[5]Department of Environment, Land and Infrastructure Engineering, Politecnico di Torino, Torino, Italy

[6]Institute of Atmospheric Sciences and Climate, Consiglio Nazionale delle Ricerche, Torino, Italy

[7]Department of Earth and Environmental Sciences, University of Milano-Bicocca, Milan, Italy

Correspondence
Anna Napoli, Department of Civil, Environmental and Mechanical Engineering, University of Trento, via Mesiano 77, 38123 Trento, Italy.
Email: anna.napoli@unitn.it

Abstract

Climate change has a strong impact on the environment in mountain areas, where ecosystems have adapted to climatic conditions that change with elevation. In this study, the response of temperature and precipitation climatic indices in the complex orography setting of the Great Alpine Region is discussed. The high-resolution gridded dataset that is presented has been produced with the Weather Research Forecasting (WRF) convection permitting regional model. Two 30-year periods have been considered (1979–2008, 2039–2068), obtained by downscaling global climate simulations with historical setting and RCP8.5 emission scenario. Both daily temperature and precipitation statistics have been found to be significantly different in the two periods, consisting in an overall projected warming and drying of the region. The dependence of the projected changes on elevation is highlighted, indicating a larger warming at medium and high elevations as well as a limited or nonexisting drying at high elevations. Physical mechanisms at the base of those differences are presented and discussed.

KEYWORDS
climate change, convection-permitting model, elevation dependent climate change, european ALPS, WRF model

1 | INTRODUCTION

Mountain environments provide vital services to human life: they sequester CO_2, they are sources of biodiversity and provide important natural resources and ecosystem services (Adler et al., 2022). More than 50% of mountain areas have an essential or supportive role for downstream regions so much so that they are

defined as the "water towers" of the planet (Viviroli et al., 2007).

Areas with complex orography have peculiar microclimates and the conditions can be quite different in nearby locations, creating narrow ecological niches that on one hand favour biodiversity and on the other are a source of ecosystem fragility and vulnerability. It thus becomes important to understand how climate is changing in these regions. The complex orography, however, hinders our ability to project local climate evolution in the future, due to its impact on the statistics of precipitation at different time scales (Formetta et al., 2022), the inadequacies in observations that are often insufficient to capture fine-scale changes, and numerical model limitations due to potentially incomplete understanding and implementation of relevant physical processes, in addition to coarse grid spacing with respect to mountainous topography. Despite these limitations, the research community agrees on the fact that mountain ecosystems are particularly sensitive to the impacts of climate change (Beniston, 2005; Beniston et al., 1997): mountains are climatic "hotspots" where change can anticipate or amplify what is occurring elsewhere, directly affecting mountain settings, but also all those who depend on them. There is growing evidence that mountain areas are responding faster and more intensely to climate change, in comparison to the global mean and to other regions (Pepin et al., 2015, 2022). In fact, a relatively small change in temperature can have major effects if it triggers nonlinear processes such as phase transitions: one of the most widely reported effects of global warming is the present and projected rapid melting of the mountain glaciers all over the world, from Himalayas (Kraaijenbrink et al., 2017; Yao et al., 2012) to the Alps (Vincent et al., 2017; Žebre et al., 2021), with cascading effects on water, biodiversity and livelihoods (Xu et al., 2009). Another expression of the sensitivity of mountain regions to climate change is the Elevation Dependent Warming (EDW), that is, a differential rate of temperature change as function of elevation. This phenomenon has been observed in many mountain areas of the world and it is projected to continue and in some cases to be significantly amplified in the future (Palazzi et al., 2017; Rangwala et al., 2013, 2016), due to the existence of a wide range of mechanisms that are possible drivers of EDW (Palazzi et al., 2019).

The European Alps represent an especially challenging region: they are one of the highest and most extensive mountain range systems in Europe. They are exposed to intense synoptic perturbations from the Atlantic and to moisture-rich inflows from the Mediterranean. The Alpine region is also influenced by both global and local anthropic activities that impact climatic conditions, as it is surrounded by highly urbanized areas. The pollution levels in the Po Valley, just south of the Alps, reach the highest values measured in the continent (Bigi et al., 2012; Bigi & Ghermandi, 2014; Fuzzi et al., 2015; Guariso & Volta, 2017). Previous studies suggest that elevation dependence of climate change in the region is affected by aerosol loads (Dhital et al., 2022; Kuhn & Olefs, 2020; Napoli et al., 2019; Pepin et al., 2015; Rangwala & Miller, 2012).

Portions of the Alps have warmed twice as much as the global average between the late 19th and the early 21st century (Auer et al., 2007; Ceppi et al., 2012), despite the fact that negative elevation-dependent warming has been found in the Eastern side of the Italian Alps over some periods of time (Tudoroiu et al., 2016). On average temperatures are expected to further rise by the end of the 21st century. This warming is projected to be particularly strong in summer, at high altitudes and on the Southern slopes of the Alps (Kotlarski et al., 2022). Observed changes of precipitation are not robust, as they show very high spatial variability (Auer & Böhm, 1994; Gobiet et al., 2014; Rysman et al., 2016; Zubler et al., 2014), although studies have shown that the distribution of annual precipitation among the lowlands and the mountains over the GAR has varied over time (Napoli et al., 2019). The studies carried out so far have shown that summer precipitation in the Alpine region is projected to be characterized by a substantial decrease on the western and southern side (Coppola et al., 2021; Kotlarski et al., 2022), and by an increase in the Eastern Alps, due to enhanced convection in that area (Dallan et al., 2021; Giorgi et al., 2016). Winter precipitation, on the other hand, is projected to increase North of the Alps, while large uncertainties and contrasting results have been reported for the Southern part (Coppola et al., 2021; Kotlarski et al., 2022). As a consequence, the Alpine area is characterized by substantial uncertainty in the position of the zero line of precipitation change, especially in the winter months (Giorgi & Coppola, 2007; Jacob et al., 2014; Kjellström et al., 2018). The overall reduction in snow cover over the Alps in the last decades has already been reported (Matiu et al., 2021; Valt & Cianfarra, 2010), and projections, depending on the emission scenario, show that Alpine glaciers will disappear to a large extent by the end of the 21st century (Žebre et al., 2021; Zekollari et al., 2019).

Due to their impacts, changes in weather extremes represent a particularly important study. The monitoring, detection and attribution of changes in extremes has been facilitated by the definition of a standard suite of indices for extreme conditions and climate change (Karl et al., 1999; Peterson et al., 2001). These indices are mainly based on daily temperature and precipitation: using regional ensembles, climate change indices have been analysed over the entire Europe (Coppola et al., 2021) and over the Alps (Kotlarski et al., 2022). Recently, the importance of studying them as a function of altitude has gained

attention (Kotlarski et al., 2012, 2015). The present study aims at complementing and extending the mentioned works by investigating projected changes in climate indices over the Great Alpine Region at convection-permitting resolution and at climate temporal scale (30 years), in order to assess and analyse elevation dependencies and physical processes at their base.

This paper is organized as follows: in the first part we describe tools, methods and datasets used for the study. In the second part the results are presented, while the last paragraph includes the discussion of the results.

2 | TOOLS AND METHODS

2.1 | Regional climate model

The Weather Research Forecasting (WRF) model (version 3.9.1.1) has been used for this study in a nonhydrostatic configuration: 30-year historical simulations (1979–2008) and climate-change projections (2039–2068) at convection permitting resolution (4 km) have been run to be able to better model the interaction between the air masses and the complex orography. The model has been run with initial and boundary conditions provided by EC-Earth global model at 0.25° grid resolution as described in Davini et al. (2017), characterized by a daily update of SST. The Representative Concentration Pathway 8.5 (RCP 8.5) has been used as global emission scenario, which is compatible with the scenario where no special measures to combat climate change are taken. This scenario estimates a global temperature increase of more than +2.5°C over pre-industrial levels by the year 2070.

The study area is the Great Alpine Region (GAR), which is represented on two nested domains (Figure 1): the outer domain is characterized by a grid spacing of 12 km, while the inner one by a grid spacing of 4 km. The outer domain includes the convection parameterization scheme by Tiedtke (Tiedtke, 1989), necessary to represent the vertical motions that characterize the summer climate in the area under analysis, not explicitly resolved at the 12 km resolution. The vertical structure of both domains consists of 50 terrain-following levels with a top pressure level set at 50 hPa. The vertical resolution is finer near the ground (order of tens of meters), while it is coarser aloft (order of several hundreds of meters). Previous studies have already used this configuration comparing results with lower-resolution models and observational datasets (Pieri et al., 2015), indicating that it is an acceptable compromise between the computational burden and the need of resolving smaller scales to predict events with small temporal and spatial scales (Adinolfi et al., 2020; Takayabu et al., 2022). The output is stored at hourly temporal resolution to allow studies based on extreme precipitation at subdaily scales, which have significant flooding impacts in rural and urban environments.

The simulations have been run with the two-way nesting approach, where the two-way interaction is reciprocal and simultaneous. The planetary boundary layer is parametrized with the Yonsei University Scheme (Hong et al., 2006). The shortwave and longwave option used is the RRTMG (Rapid Radiative Transfer Model for Global) (Iacono et al., 2008): with this scheme, the CAM Green House Gases (GHG) option has been activated. This option provides annual GHGs from 1765 to 2500 so that the RRTMG long-wave scheme interacts with GHGs. The Thompson Aerosol-Aware microphysics scheme has been used (Thompson & Eidhammer, 2014): this microphysics parametrisation has an explicit nucleation of water droplets and activation of ice by dynamical aerosols. Aerosols are advected, interact with clouds and with radiation and are input at the surface through a flux which is time independent (and thus with no difference between the historical and the scenario simulations) but surface-elevation dependent (larger flux in lowlands and smaller at high altitudes). The parameter values used in the simulations are reported in Data S1, Supporting Information.

2.2 | Climate extreme indices

For the objective measurement and characterization of the variability and change of extremes with altitude, a suite of the international climate change indices ETCCDI (http://etccdi.pacificclimate.org/list_27_indices.shtml) has been used and studied. The set of climate indicators on which the analysis is based includes indices that represent the main weather-induced impacts on the natural, social and economic spheres. In this work, some modifications were applied to the selected indicators to take into account the specificities of the Alpine territory and the aim of this study. The indices are:

- Tmean: seasonal mean temperature.
- FD5P: mean annual number of days with minimum daily temperature below the 5th percentile of the historical run.
- SU95P: mean annual number of days with maximum daily temperature greater the 95th percentile of the historical run.
- Seasonal precipitation: seasonal mean precipitation.
- R20: mean number of days with daily precipitation greater than 20 mm.
- R95pTOT: annual average of the cumulative precipitation that is above the 95th daily historical percentile on a wet day (RR ≥ 1 mm), where RR is the daily mean precipitation.
- CDD: annual mean of the maximum number of consecutive days with less than 1 mm·day^{-1} of rain.
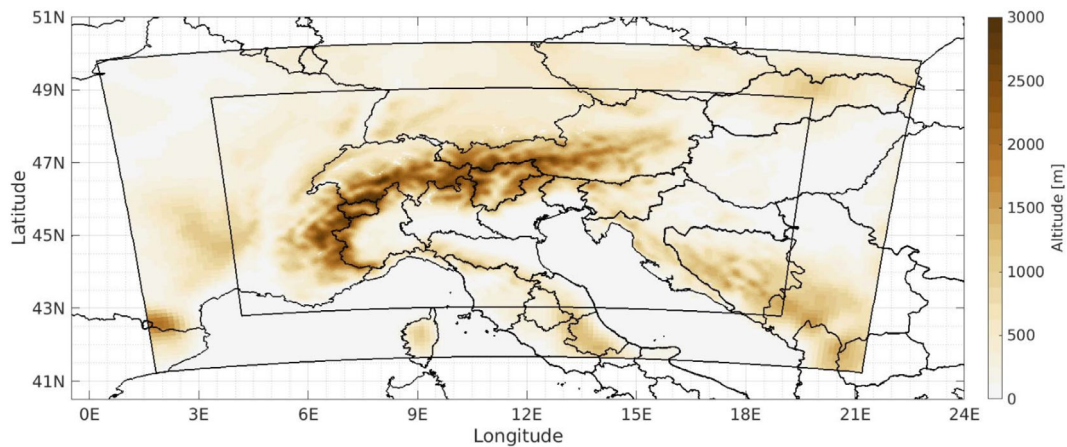
FIGURE 1 Two grafted domains that represent the GAR used in this model study. The topography of the inner domain (4 km resolution) and of the external domain (12 km) are represented [Colour figure can be viewed at wileyonlinelibrary.com]

Maps of the indices for historical simulation and climate projection, as well as of their difference, have been produced. Climatological conditions of the indices are shown in Data S2. Moreover, land data have been clustered according to surface elevation in order to evidence the existence of altitudinal dependences in the change of the indices. In particular, land positions over the GAR are divided into 18 elevation classes, where the class limits are chosen so that each class has the same number of pixels (the class limits result in about 0–75, 75–114, 114–149, 149–190, 190–233, 233–277, 277–325, 325–382, 382–446, 446–508, 508–584, 584–675, 675–791, 791–930, 930–1114, 1114–1378, 1378–1856 and 1856–3062 m). We then compute the mean of the projected-historical index change for each class, and verify whether there is any statistically significant dependence of the index change versus elevation. The statistical significance is evaluated based on the rejection of the null hypothesis of no relationship of index change with elevation (obtained using repeated shuffling with 5000 permutations).

2.3 | Validation of the model dataset

To validate the climate dataset produced with the above described simulations, comparisons with different datasets have been carried out: E-OBS, APGD, ERA5 and ERA5_LAND.

The observational dataset E-OBS version 23.1 at about 11 km (0.1° × 0.1°) resolution (https://surfobs.climate.copernicus.eu/dataaccess/access_eobs.php) has been used to evaluate temperature and precipitation variables. With a different gridding procedure compared to the previous version (Haylock et al., 2008), this new version of E-OBS provides daily gridded land-only observational dataset over Europe. In this version a 100-member ensemble of each daily field has been generated (Cornes et al., 2018). Since the initial construction of E-OBS (Haylock et al., 2008), many more station series have been added: during the 90s, precipitation stations were about 7000, while temperature stations were about 3000 over the entire Europe with a large density over Germany and Scandinavia regions (Cornes et al., 2018). This spatial distribution of stations resulted in an increasing disparity in station density across the domain, with relatively many stations in Central Europe and Scandinavia, and many fewer toward the South and East of the domain (Mediterranean and Alpine area). This low density of stations over the complex orography area has an impact over the thermodynamical variables and it increases the uncertainty of the data in the area of interest (Hofstra et al., 2009).

The EURO4M-APGD dataset (Isotta et al., 2014) has been used to validate precipitation: the dataset is based on a collection of high-resolution rain-gauge data from seven Alpine countries (about 5500 measurements per day) in the period 1971–2008. The dataset is characterized by a grid spacing of 5 km, daily time resolution, and it was constructed with a distance-angular weighting scheme that integrates climatological precipitation–topography relationships.

The latest version of ERA5 at 0.25° (about 27 km) has been used for the precipitation variable (Hersbach et al., 2020): ERA5 provides hourly estimates of a large number of atmospheric, land and oceanic climate variables. The data cover the Earth and resolve the atmosphere using 137 levels from the surface up to a height of 80 km. ERA5 includes information about uncertainties for all variables at reduced spatial and temporal resolutions. Quality-assured monthly updates of ERA5 (1979 to present) are published within 3 months of real time. To

obtain more robust statistics, the ERA5_LAND dataset has also been used to validate the temperature variable: it contains an orographic bias correction based on the lapse rate and it is characterized by a spatial resolution of 9 km (Muñoz-Sabater et al., 2021).

Temperature and precipitation datasets from WRF, E-OBS, ERA5 and APGD (for precipitation) and ERA5_-LAND (for temperature) have been interpolated on a common grid, chosen as the coarser grid available, that is, E-OBS grid for temperature ($0.1° \times 0.1°$), ERA5 grid for precipitation ($0.25° \times 0.25°$). A first-order conservative remapping method (Jones, 1999) has been used for precipitation and temperature variables, a method chosen for its ability in preserving spatial integrals of the data between the source and target grids.

To investigate the seasonality in the results, four time periods have been separately analysed: December–January–

February (DJF), March–April–May (MAM), June–July–August (JJA) and September–October–November (SON).

Table 1 shows the climatological temperature of the regridded datasets averaged over land points in the entire domain, together with its spatial standard deviation: the WRF dataset is characterized by a larger spatial variability compared to ERA5_LAND and E-OBS with a slightly higher mean summer temperature and a slightly lower mean winter temperature.

Figure 2 shows the spatial distribution of the difference between the seasonal mean temperature between the WRF dataset and E-OBS: in lowlands, WRF temperatures are typically lower than E-OBS temperatures during winter and higher during summer, while the highest elevations have a consistent bias through the year, with colder temperatures in WRF than in observations in every season and a particularly large temperature difference in the Alps in winter, a pattern that is in line with past modelling work on km-scale temperature over the Alps (Leutwyler et al., 2017). Figure 3 shows the probability density functions (pdfs) of climatological mean temperature for the three different regridded datasets: in most cases temperature pdfs from WRF model have heavier tails than in the other datasets, especially for extremely low values. This finding is consistent with the fact that the high-resolution WRF model produces fields on a finer grid and at times at higher elevation, whereas in coarser resolution datasets the values are smoothed

TABLE 1 Mean temperature (1979–2008) over the entire domain and the corresponding spatial standard deviation for three different datasets

	WRF (°C)	ERA5_LAND (°C)	EOBS (°C)
DJF	−0.51 ± 3.86	0.01 ± 3.54	0.86 ± 2.89
MAM	8.41 ± 4.18	8.20 ± 3.51	8.77 ± 3.42
JJA	19.13 ± 4.00	17.78 ± 3.49	17.90 ± 3.60
SON	9.47 ± 3.46	9.51 ± 3.19	9.71 ± 3.05
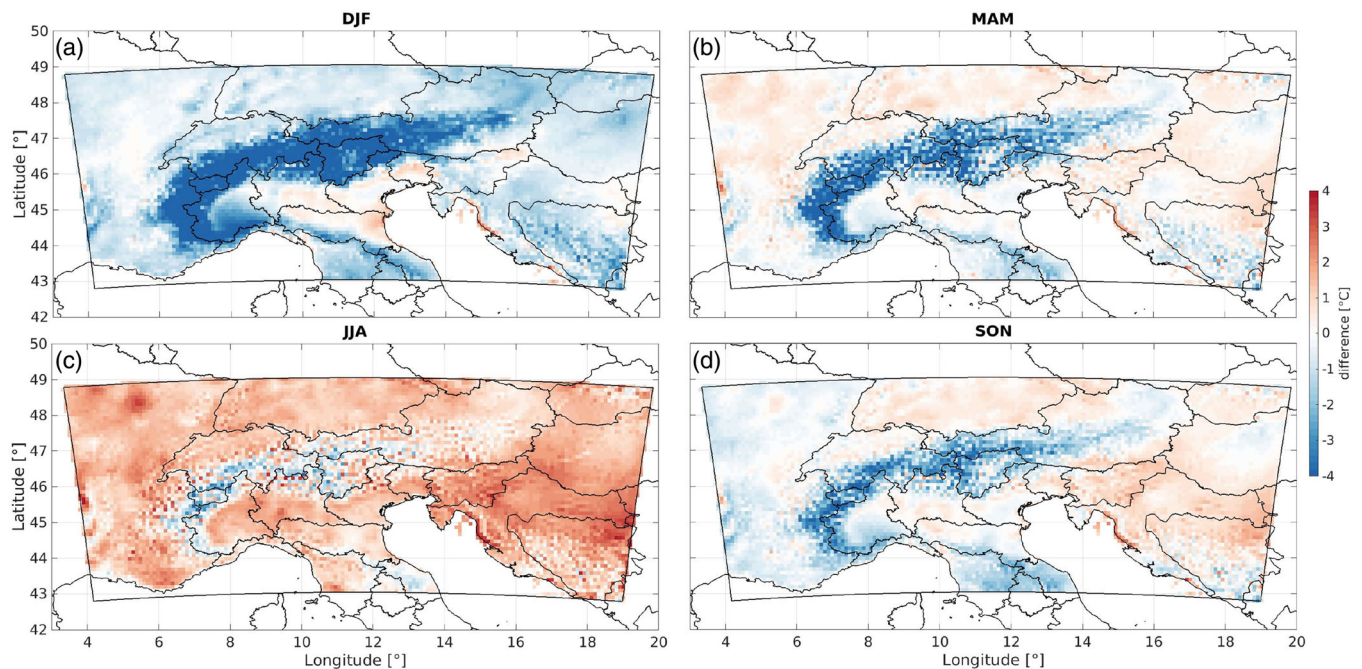
FIGURE 2 Difference in the daily mean temperature between WRF-historical and E-OBS dataset (climatologies over the period 1979–2008), for the different seasons. WRF has been interpolated over the E-OBS grid using the bilinear method [Colour figure can be viewed at wileyonlinelibrary.com]
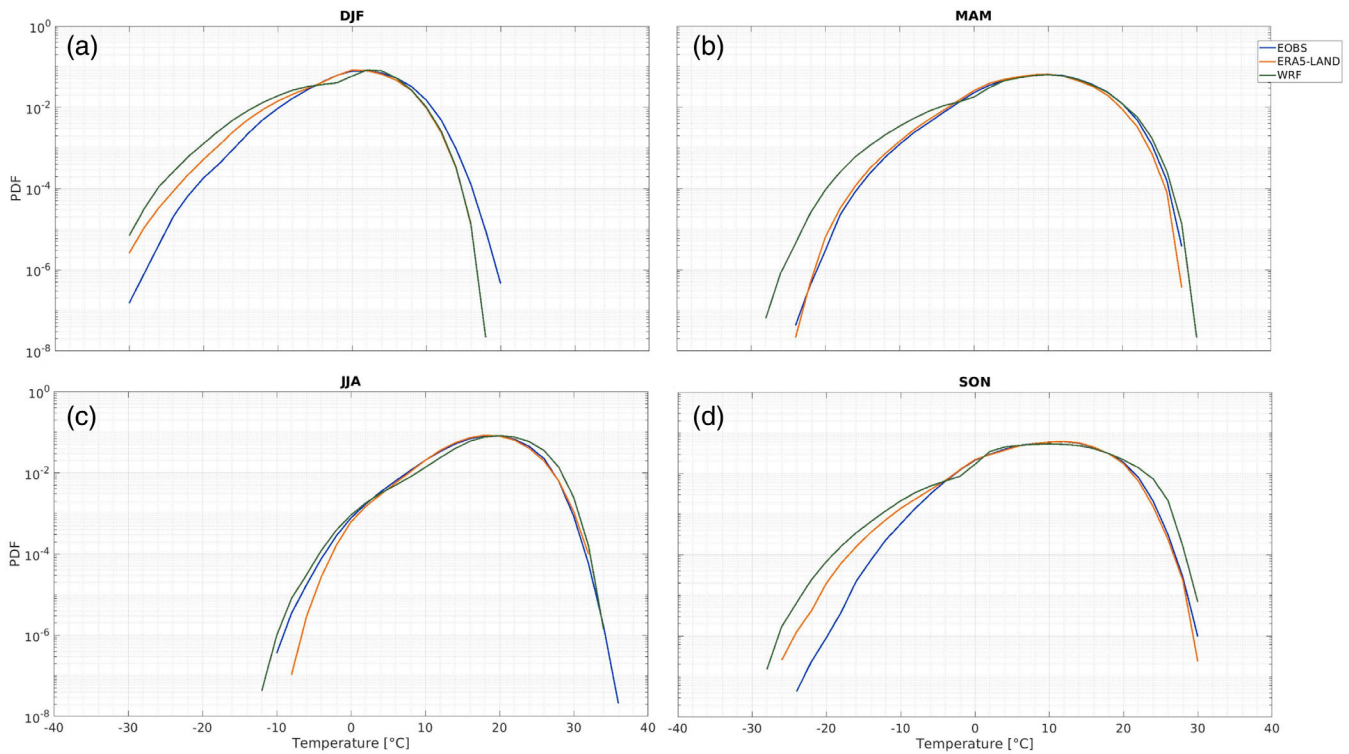
FIGURE 3 Pdf of seasonal mean temperature of three different datasets (1979–2008) all interpolated over the E-OBS grid space: WRF-historical (green line), ERA5_LAND (orange line) and E-OBS (blue line) [Colour figure can be viewed at wileyonlinelibrary.com]
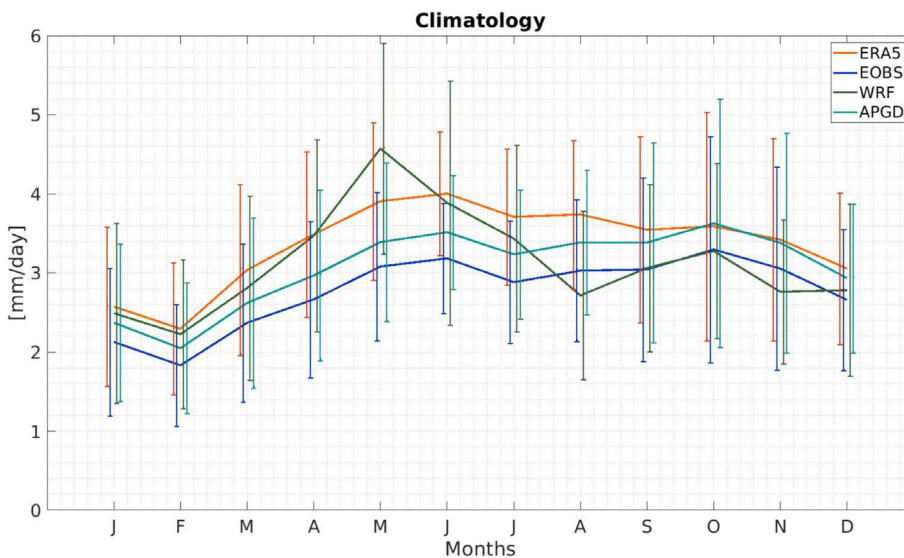

FIGURE 4 Monthly mean precipitation averaged over the GAR (1979–2008). Datasets are all interpolated over the ERA5 grid space. Error bars represent the interannual variability of the mean monthly precipitation over the entire domain (standard deviation) [Colour figure can be viewed at wileyonlinelibrary.com]

over a relatively large grid box and extreme values are less frequently encountered. Despite those differences, the seasonality of the temperature field is well reproduced in WRF dataset.

Monthly climatologies of precipitation over the GAR are shown in Figure 4. The seasonal cycle of precipitation has a larger amplitude in WRF than in the other datasets, mainly due to a wetter spring season than in both

reanalysis and observational products. With respect to ERA5, WRF is drier during most of the year (except for May), with largest rainfall differences (up to −17%) during fall and winter season, when however ERA5 is wetter than E-OBS and APGD. When analysing the seasonal precipitation difference maps (Figure 5), it becomes evident that rainfall differences with respect to the reanalysis are not homogeneous over the entire domain and that
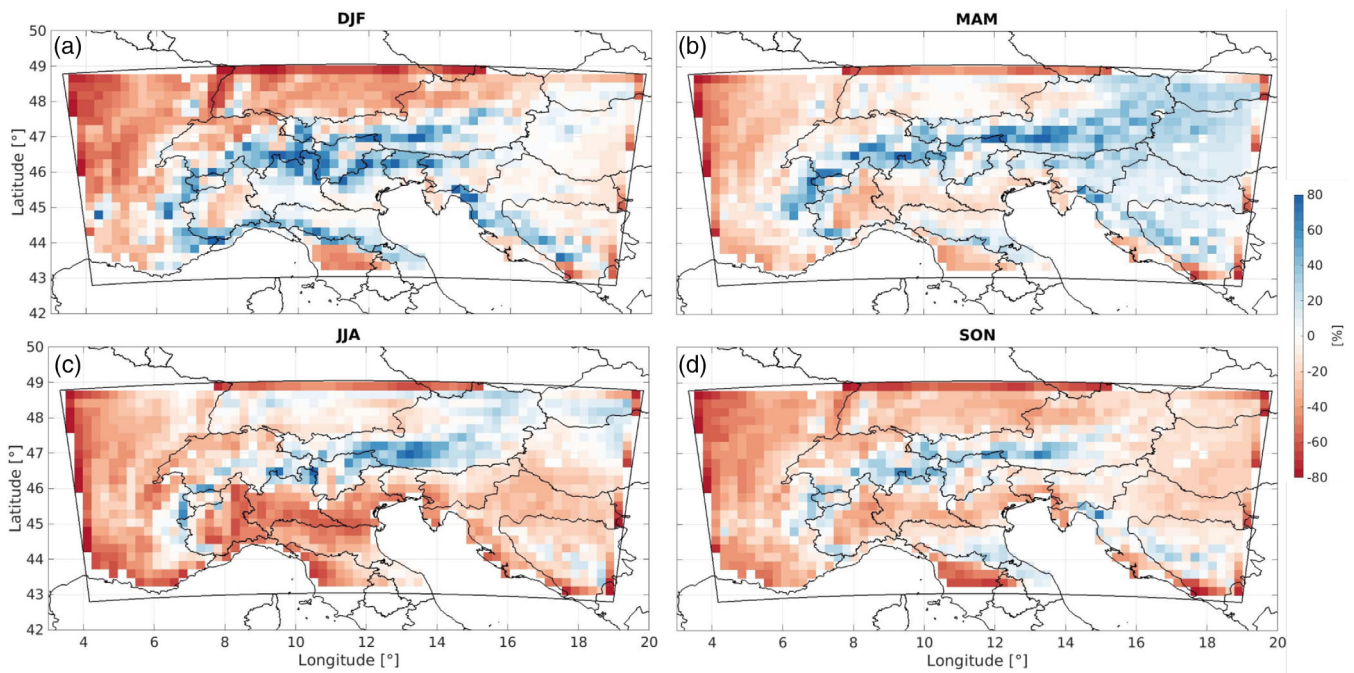
FIGURE 5 Difference (in percentage) of mean seasonal precipitation between WRF-historical and ERA5 (1979–2008). WRF data has been interpolated onto the ERA5 grid [Colour figure can be viewed at wileyonlinelibrary.com]
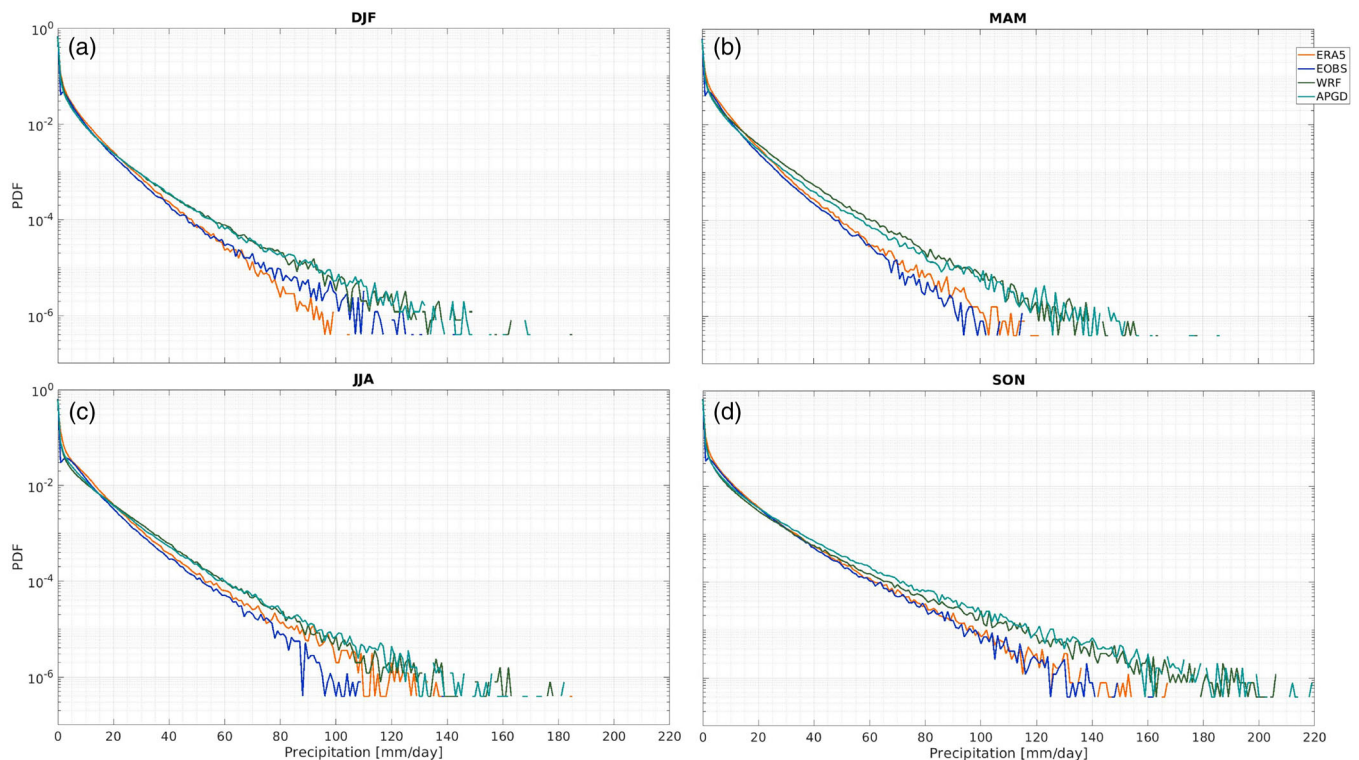

FIGURE 6 Probability density functions of the daily precipitation in each season (climatology over 1979–2008): WRF-historical (green line), ERA5 (orange line), E-OBS (blue line), APGD (light blue line). All datasets have been interpolated onto the ERA5 grid [Colour figure can be viewed at wileyonlinelibrary.com]

the high-elevation areas are consistently wetter in WRF than in ERA5 in every season. This result is in agreement with previous studies that compared high-resolution models with observational and reanalysis datasets in region with complex terrain (Ban et al., 2021; Kotlarski et al., 2014; Pieri et al., 2015; Smiatek et al., 2016).
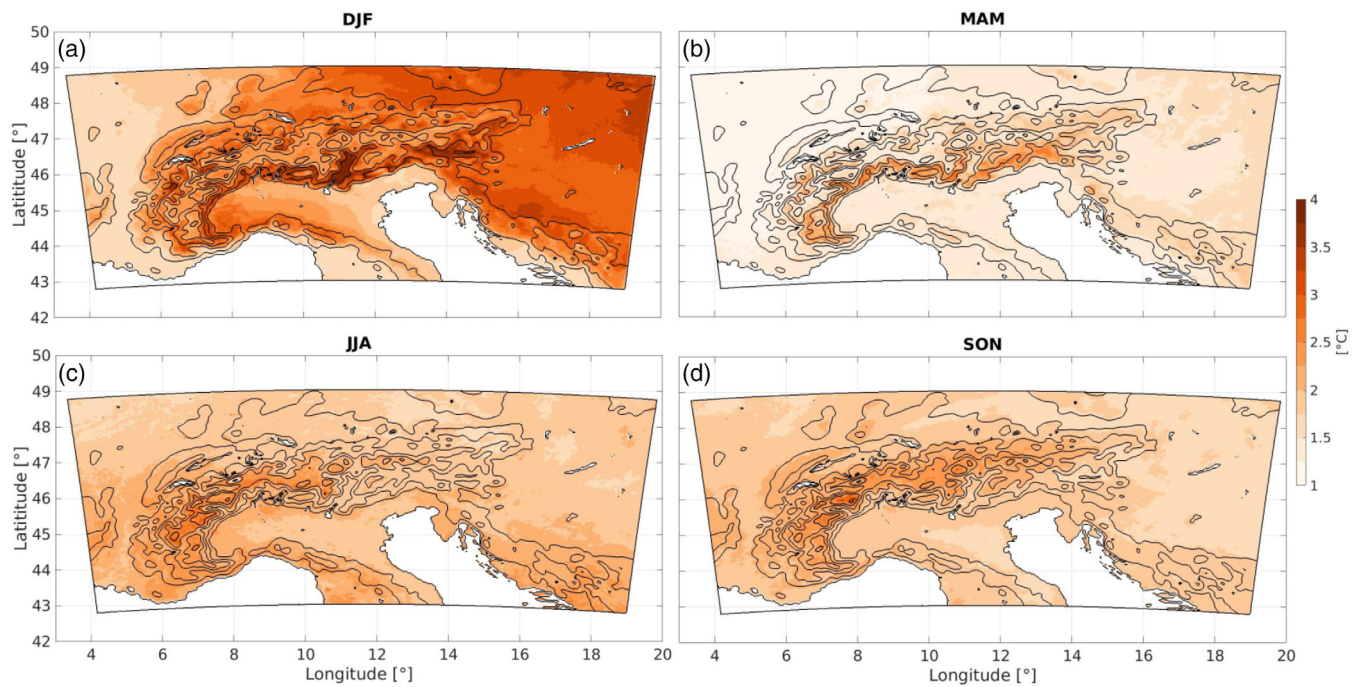
FIGURE 7 Map of the difference between future (2039–2068) and historical WRF simulation (1979–2008) in seasonal mean 2 m temperature: DJF (a), MAM (b), JJA (c) and SON (d). Isolines represent the elevation every 500 m [Colour figure can be viewed at wileyonlinelibrary.com]

The distributions of the probability density functions for the daily rainfall rate on the GAR domain are shown in Figure 6: WRF and APGD have similarly higher probabilities of extreme values compared to E-OBS and ERA5 in all seasons, in line what the expectations, given that the data in E-OBS and ERA5 have a coarser effective resolution. Despite the comparison has been performed on the same grid, the lack of high-resolution data to generate E-OBS and ERA5 datasets limits their capability of reproducing precipitation extremes (Ban et al., 2021; Pichelli et al., 2021; Pieri et al., 2015).

3 | PROJECTED CHANGE IN CLIMATE EXTREME INDICES

In this section, the differences between future projections and historical time period are presented for each index.

Temperature indices show that the GAR is characterized by a projected rise in temperature with an inhomogeneous warming rate over the domain (Figure 7). The altitudinal dependence of the temperature increase is shown in Figure 8, indicating that over the mountains there is an enhanced warming rate. A particularly large warming is also present during winters in the low-elevation northeastern part of the domain. These signals can be related to snow melting and the ice-albedo feedback (Gobiet et al., 2014): regions with historical seasonal

temperatures close to the freezing point experience a significant increase in solar radiation absorption due to snow melt in a warmer world. Both the northeastern part of the domain (in winter, when mean temperatures vary between −1°C and +1°C; see Figure S16b) and the area around the snow equilibrium line over the mountains (which depends on the season) have a higher sensitivity to increased greenhouse gasses than the rest of the region (Frei et al., 2018; Žebre et al., 2021). Indeed, the peak in temperature increase is found at elevations between 1000 and 1500 m in winter (Figure 8a), slightly above 1500 m in spring (Figure 8b), and in the highest elevation band in summer and fall (Figure 8c,d), in line with the given interpretation.

In order to assess the projected change of extreme temperatures, particularly relevant for impact studies, we also computed the changes in minimum and maximum daily temperatures. The projected change in the mean number of frost days (minimum temperature below 0°C) shows a large decrease in the plain and a minimal variation at high elevations (Figure S14); the low sensitivity in the number of frost days at high altitudes is associated with the fact that the minimum temperature is often substantially lower than 0°C, thus not particularly sensitive to the projected warming. The projected change in the mean number of summer days (maximum temperature above 25°C) increases by about 15% at low elevations and more at higher elevations, with more than a doubling at
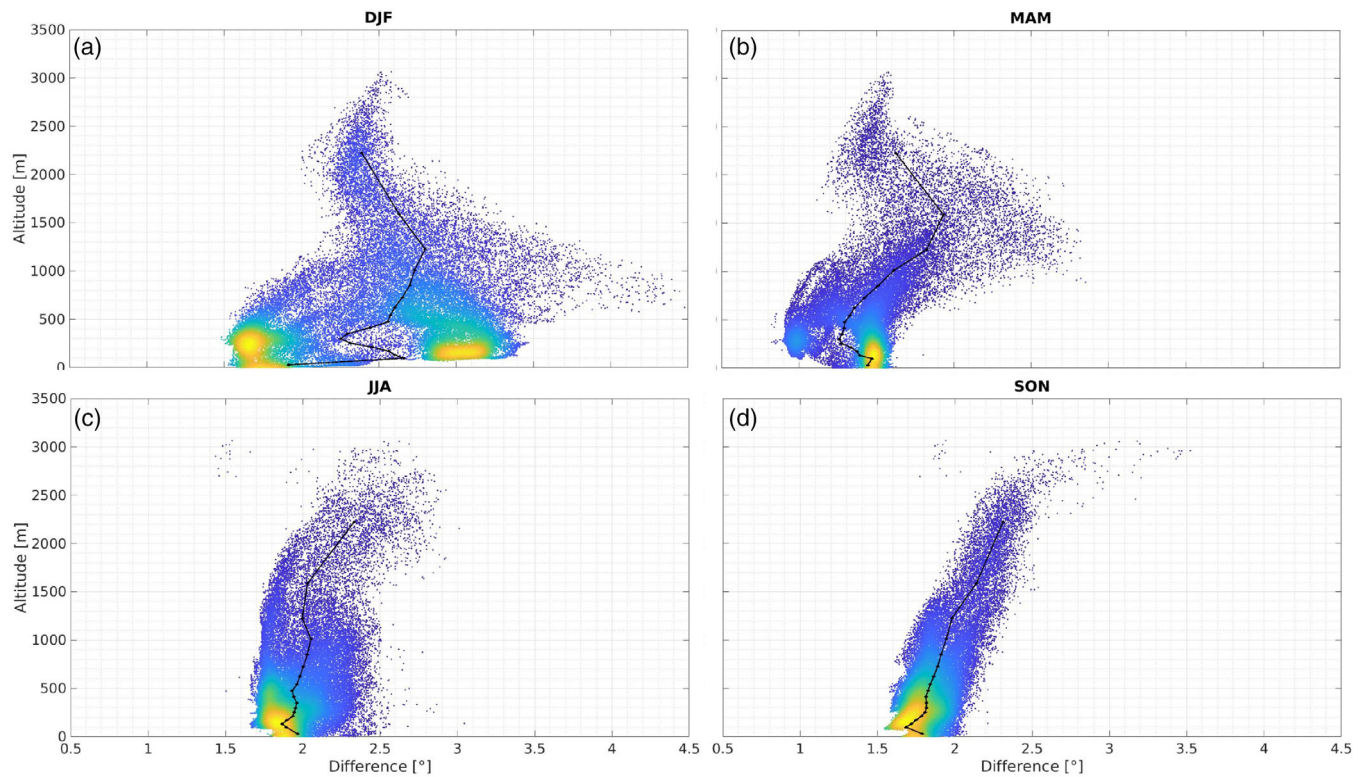
FIGURE 8 Scatter plot of the difference in the seasonal mean 2 m temperature between future projections (2039–2068) and historical simulations (1979–2008) in function of altitude. Colours represent the density of the points in the GAR from yellow (high density) to blue (low density). The mean is calculated and plotted for each band of altitude (black points). Spring, summer and autumn are characterized by a significant elevation dependence of about $+0.24°C\cdot km^{-1}$ in spring (b), $+0.15°C\cdot km^{-1}$ in summer (c) and $+0.25°C\cdot km^{-1}$ in fall (d) [Colour figure can be viewed at wileyonlinelibrary.com]

about 1000 m (Figure S15). In order to evaluate the change in local extreme temperatures we also computed FD5P and SU95P indices, which are based on locally defined thresholds. Defined as the number of days with minimum temperature below the local historical 5th percentile (FD5P) and maximum temperature above the local historical 95th percentile (SU95P), the projected reduction of FD5P (Figure 9a) and increase of SU95P (Figure 10a) are both indicative of warming (they respectively correspond to an increase of minimum and of maximum daily temperatures), in agreement with previous studies (Kjellström et al., 2018; Russo et al., 2015). It is interesting to note that there is an altitudinal dependence in such changes, as shown in Figures 9 and 10: the number of days with minimum daily temperatures below the locally defined threshold decreases at relatively low elevations more than at high elevations, while the number of days with high maximum daily temperatures increases at high elevations more than at low elevations. In other words, summer peak temperatures increase more over mountains (where there is nearly everywhere a doubling in the number of hot days), in line with the projected changes of mean temperature, while very cold winter

nights tend to disappear in areas particularly sensitive to snow melt, characterized by a large change in albedo (Figure S16).

Maps of the seasonal precipitation projected changes are represented in Figure 11: summer precipitation is projected to decrease over the whole domain, with some exceptions at high altitudes where some areas have a positive variation compared to the historical period. In winter a strong dipole is present, with the mountain range acting as a dividing line: to the North of the Alps winter precipitation is projected to increase while to the South the opposite signal emerges. Spring and autumn are characterized by less intense changes in precipitation, with a slight decrease in the Po Valley contrasted by seasonally variable behaviour in the Alps. Figure 12 shows the elevation dependence of the seasonal precipitation: spring season shows a statistically significant elevation dependence characterized by values close to zero at lowlands and values close to +10% at high altitudes. During winter and summer there is a significant drying at low elevations (about −18% in both seasons) and a small change to total precipitation at higher elevations (about −10% in summer and +8% in winter). Overall, the projected
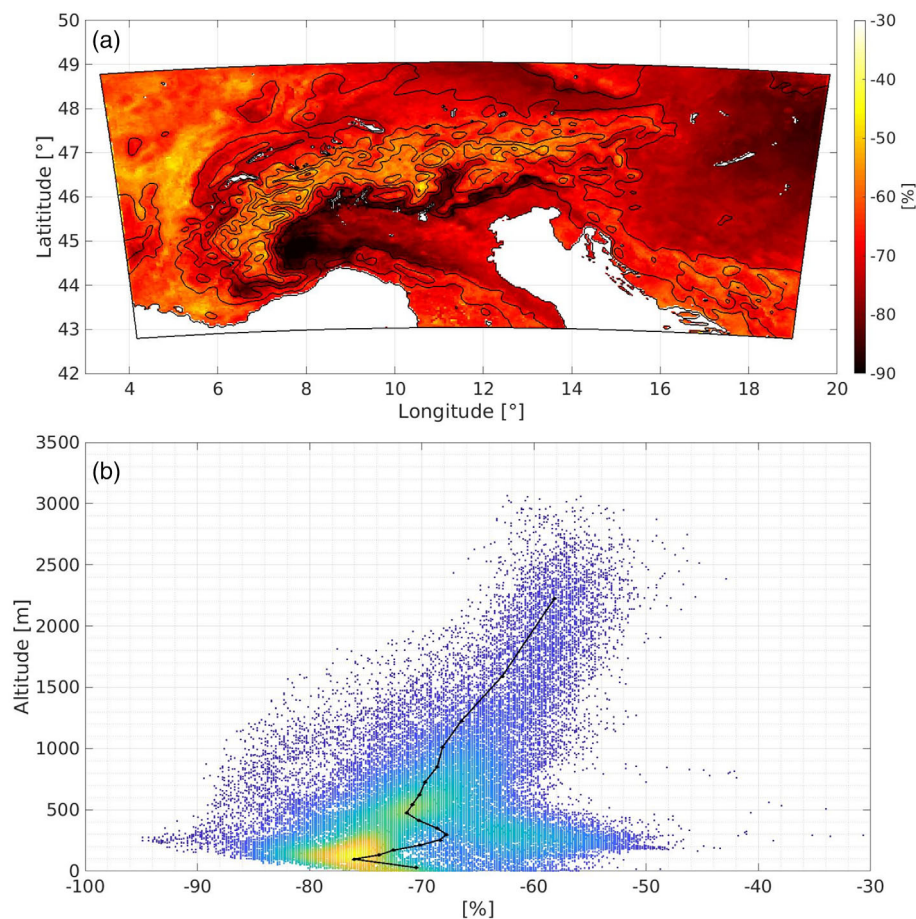
FIGURE 9 Relative change to the number of cold days (FD5P) between projected (2039–2068) and historical WRF runs (1979–2008): (a) map, and (b) scatter plot as a function of altitude. In (a) isolines represent the elevation every 500 m. In (b) colours represent the density of the points in the GAR from yellow (high density) to blue (low density). The mean is calculated and plotted for each band of altitude (black points). The elevation dependence is significant at 95% confidence level ($+6.00\%\cdot km^{-1}$) [Colour figure can be viewed at wileyonlinelibrary.com]
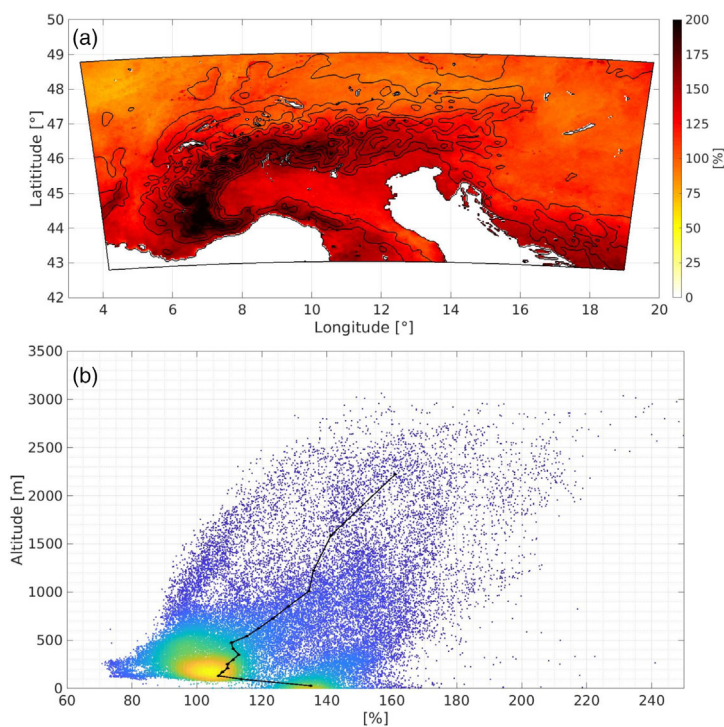

FIGURE 10 Relative change to hot days (SU95P) between projected (2039–2068) and historical WRF runs (1979–2008): (a) map and (b) scatter plot as a function of altitude. In panel (a) isolines represent elevation every 500 m. In panel (b) colours represent the density of the points in the GAR from yellow (high density) to blue (low density). The mean is calculated and plotted for each band of altitude (black points and error bars). The elevation dependence is statistically significant and it is about $+22\%\cdot km^{-1}$ [Colour figure can be viewed at wileyonlinelibrary.com]

change in annual mean precipitation shows a main reduction over the GAR, where a small increase is present only over mountains located on the Northern side of

the Alps (Figure S17). The possible explanations for precipitation change patterns will be further explored in the section 4.
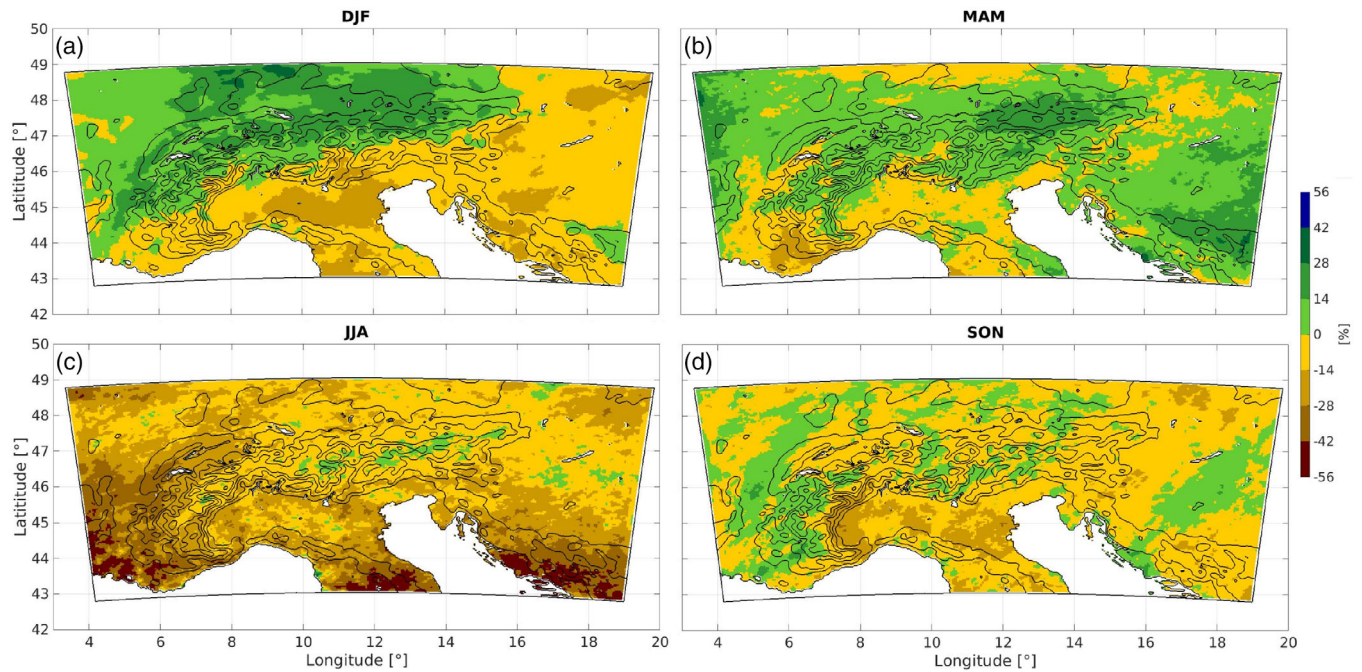
FIGURE 11 Map of the relative change to mean seasonal precipitation between projected (2039–2068) and historical WRF runs (1979–2008): winter (a), spring (b), summer (c) and fall (d). Isolines represent the elevation every 500 m [Colour figure can be viewed at wileyonlinelibrary.com]
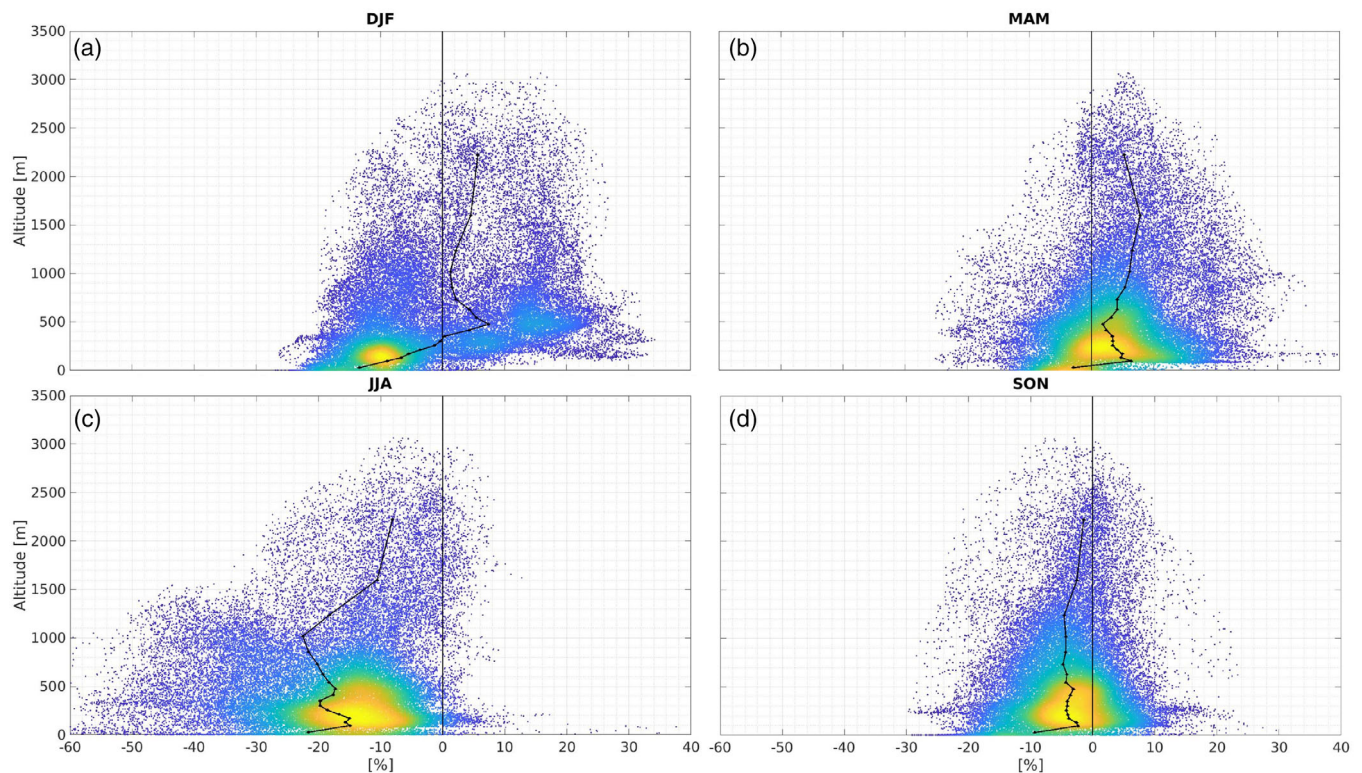
FIGURE 12 Maps of the relative change to seasonal precipitation, shown as function of altitude: DJF (a), MAM (b), JJA (c) and SON (d). Colours represent the density of the points in the GAR from yellow (high density) to blue (low density). The mean is calculated and plotted for each band of altitude (black points). The elevation dependence is not significant in autumn, while in summer (+3.0%·km^{-1}), spring (+2.0%·km^{-1}) and winter (+3.25%·km^{-1}) the trend with the altitude is statistically significant at 95% confidence level [Colour figure can be viewed at wileyonlinelibrary.com]
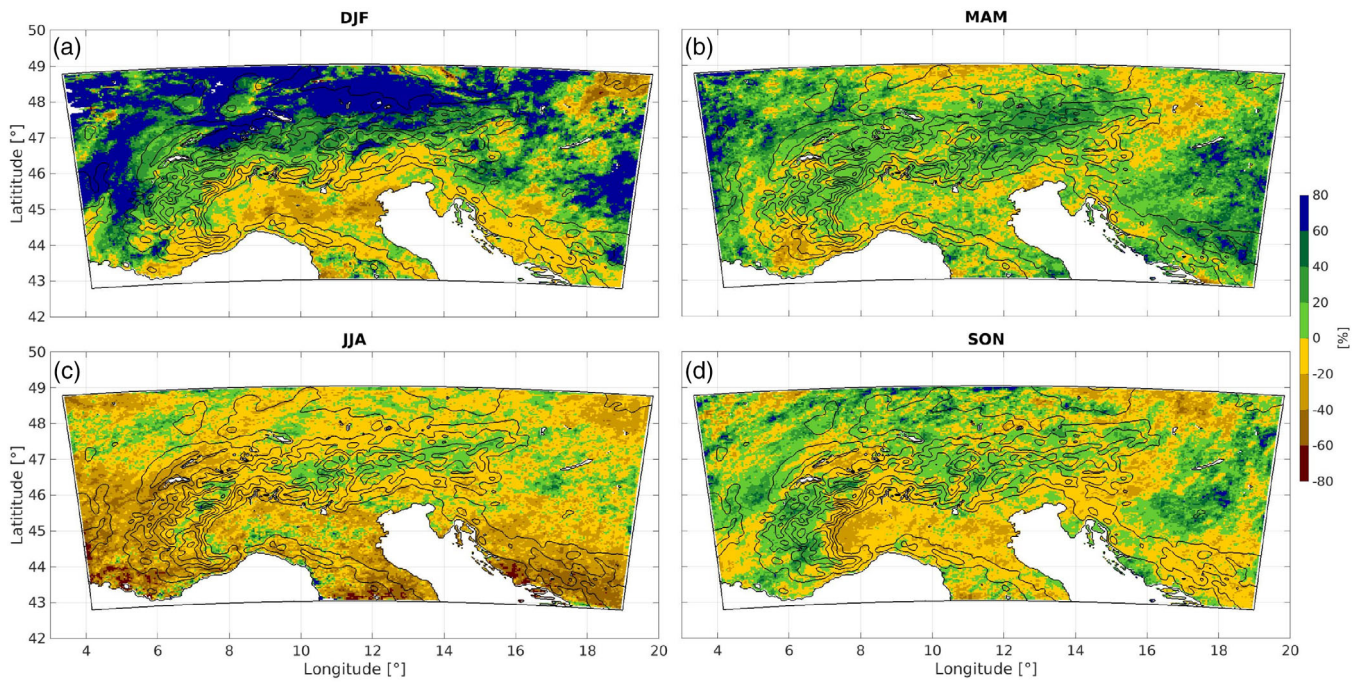
FIGURE 13 Maps of the relative change to the mean number of days with daily precipitation greater than 20 mm (R20 index): DJF (a), MAM (b), JJA (c) and SON (d). Isolines represent the elevation every 500 m [Colour figure can be viewed at wileyonlinelibrary.com]
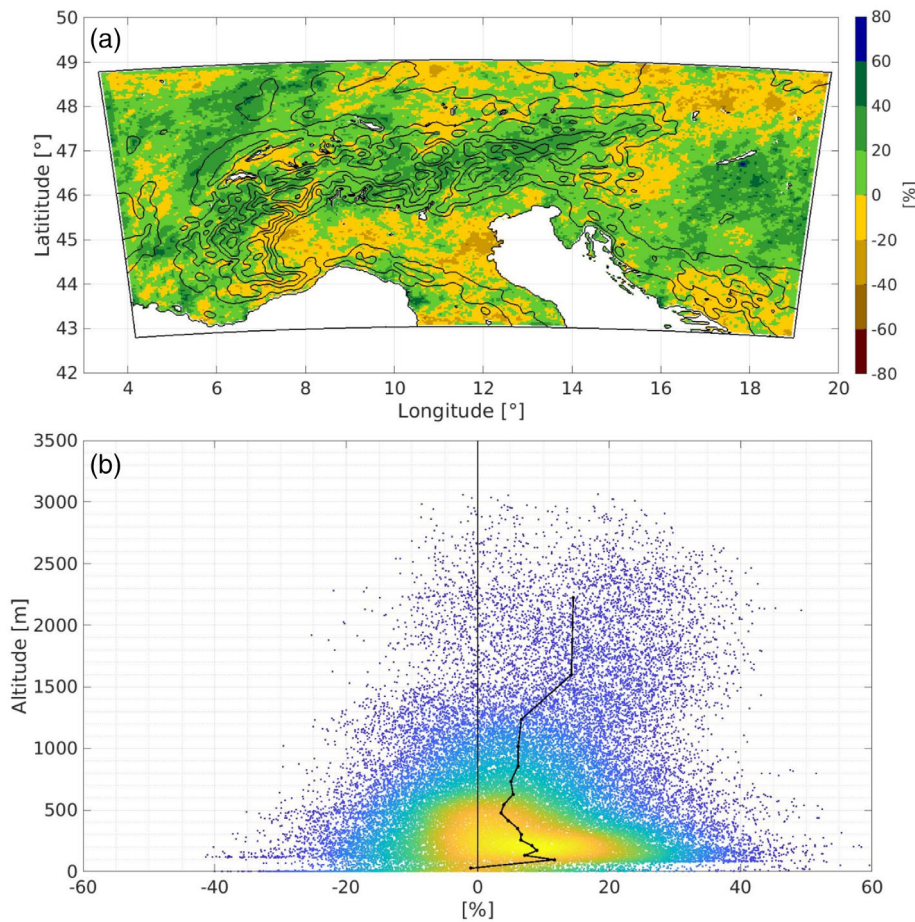
FIGURE 14 Relative change to the annual average of the cumulative precipitation that is above the 95th daily historical percentile on wet days (RR ≥ 1 mm) (R95pTOT index): (a) map and (b) scatter plot as a function of altitude. In panel (a) isolines represent elevation every 500 m. In panel (b) colours represent the density of the points in the GAR from yellow (high density) to blue (low density). The mean is calculated and plotted for each band of altitude (black points). The elevation dependence is statistically significant and it is about $+3.6\%\cdot km^{-1}$ [Colour figure can be viewed at wileyonlinelibrary.com]

FIGURE 15 Relative change to the climatological average maximum number of consecutive dry days per year (1979–2008, 2039–2068), CDD index [Colour figure can be viewed at wileyonlinelibrary.com]
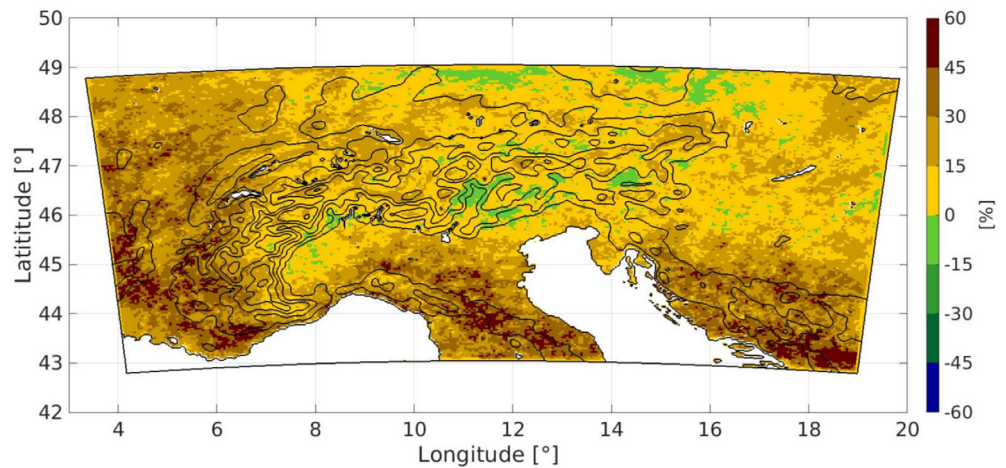
The occurrence of moderate and heavy daily rainfall events (R20 index) is projected to change in line with the change in mean precipitation (Figures 11 and 13). The elevation dependence is not statistically significant at seasonal and annual time scale (see Data S3 and Figures S18b and S19).

The intensity of extreme daily precipitation (R95pTOT index) is projected to slightly increase (Figure 14), but large differences are found across the region and also seasons (see Data S3 and Figure S20). Statistically significant elevation dependent changes are found at annual time scale (Figure 14b), while in the seasonal study only fall is characterized by a weak positive dependence on elevation (see Figure S21d).

Previous works indicated that Southern Europe is most probably facing an increased drought stress (Coppola et al., 2021; Gobiet et al., 2014), while Northern Europe is facing increased risk of intensified wet events (Coppola et al., 2021; Heinrich & Gobiet, 2012). In Figure 15 the relative change map to the climatological maximum number of consecutive dry days in a year (daily precipitation less than 1 mm, CDD index) is shown: the entire area is characterized by an increase in consecutive dry days with increasing dryness in the South of the domain. No significant elevation dependent change emerges (Figure S22).

4 | DISCUSSION AND CONCLUSIONS

Climate change has been shown to have an elevation dependence both in temperature (Palazzi et al., 2019; Pepin et al., 2015) and in precipitation (Kotlarski et al., 2015; Pepin et al., 2022). Data analysis indicates that mountainous regions can have a local response to global forcing that differs from the regional response.

In this study the imprints of projected climate change in the GAR in the mid of the 21st century have been investigated, by using, for the first time, a convective permitting model over a period of 30 years. This setup allows the evaluation of climate variations not only at the regional scale, but also at local scales, accounting for the complex orography.

The downscaling of historical and projected climate simulations demonstrates that, in the GAR, climate change has different signatures in lowlands and highlands: while historical climatologies show that temperature and precipitation are characterized by certain elevation dependent patterns (see Data S2), in future these patterns could change. Overall, Europe and especially the Mediterranean region will experience warmer temperatures and more heat waves (Kjellström et al., 2018; Russo et al., 2015), with a particularly large warming over the northeastern region, in line with past studies (Coppola et al., 2021). In this work, it is also shown that the projected warming is larger at medium and high elevations, possibly as an effect of the snow-albedo feedback. The whole region is projected to experience a reduced annual mean precipitation, but while the Po Valley presents a drying over all seasons, the Alpine arc has much smaller variations of seasonal precipitation with respect to the historical period. Similarly, the number of consecutive dry days is projected to increase over large areas, especially in the Mediterranean climate, but not particularly over the Alps. Whereas the overall projected drying is typically attributed to large scale dynamical and thermodynamical changes (de Vries et al., 2022), previous studies over the Alps (Giorgi et al., 2016) and over the Carpathians (Torma & Giorgi, 2020) discuss how the high-elevation precipitation change can be associated to the larger surface warming, which tends to destabilize the air column and favour convection.

Winter precipitation, greatly impacted by the position of the storm track, in our simulations is projected to

increase on the Northern side of the Alps and decrease on the Southern side. This dipolar change is currently debated and not fully understood (Coppola et al., 2021; Rajczak & Schär, 2017; Tramblay & Somot, 2018), but probably it is affected by longer term variability patterns such as the North Atlantic Oscillation, which is known to shift the position of the storm track (Brugnara & Maugeri, 2019; Hurrell & Deser, 2010). Preliminary analyses to investigate the impact of NAO on the projected changes of winter precipitation have been performed and are reported in Data S4, but they did not unveil the origin of the dipolar change in winter rainfall. Despite the difficulty in constraining the large scale winter precipitation change, which would certainly require the use a large ensemble modelling approach, in this study we show that the derivative of winter precipitation change with altitude is positive on both sides (see Data S4), indicating that local processes even in wintertime increase the orographic precipitation enhancement with respect to the low-elevation precipitation. Further analysis will be performed to investigate the role of air column stability and convection in this signal.

The results presented underline the importance of performing high-resolution simulations, such that the complex orography patterns as well as the convective dynamics can be well represented. This clearly leads to large computational costs. For this reason we performed and analysed only one realization of the RCM (WRF) forced with only one GCM (EC-Earth) in the historical period and in a single RCP scenario (RCP8.5). This is a clear limitation of the study, especially for projected precipitation changes, as storminess is known to have very large interannual variability and dependence on the characteristics of the atmospheric models (Feser et al., 2015). However, the robustness of the enhanced orographic precipitation signal in the projected climate, regardless of the precipitation change at low elevations, gives confidence to the relevance of the effects of local processes on elevation dependent climate change. Amplified warming over the mountains and enhancement of orographic precipitation are the main indications coming out of this study, and future work will shed light on the thermodynamical and dynamical processes at their base. The same simulations offer a wealth of information that was not investigated in the present study. Further analysis will be performed to investigate the projected response in other meteorological variables particularly important for local communities and administrators, such as snowfall and near-surface winds, and in subdaily statistics, especially interesting for describing properties of convective events (Ban et al., 2021; Kahraman et al., 2021; Pichelli et al., 2021). All data are available for other studies upon request.

AUTHOR CONTRIBUTIONS
Anna Napoli: Formal analysis; data curation; writing – original draft; writing – review and editing; investigation; methodology; visualization. **Antonio Parodi:** Writing – review and editing; investigation; methodology; visualization; writing – original draft. **Jost von Hardenberg:** Writing – review and editing; investigation; methodology; visualization; writing – original draft. **Claudia Pasquero:** Writing – review and editing; conceptualization; investigation; methodology; visualization; writing – original draft.

CONFLICT OF INTEREST STATEMENT
The authors declare no conflicts of interest.

ORCID
Anna Napoli https://orcid.org/0000-0002-5122-6363

REFERENCES
Adinolfi, M., Raffa, M., Reder, A. & Mercogliano, P. (2020) Evaluation and expected changes of summer precipitation at convection permitting scale with COSMO-CLM over Alpine space. *Atmosphere*, 12(1), 54.

Adler, C., Wester, P., Bhatt, I., Huggel, C., Insarov, G., Morecroft, M. et al. (2022) Cross-chapter paper 5: mountains. In: *Climate change 2022: impacts, adaptation, and vulnerability*. Cambridge: Cambridge University Press.

Auer, I. & Böhm, R. (1994) Combined temperature–precipitation variations in Austria during the instrumental period. *Theoretical and Applied Climatology*, 49(3), 161–174.

Auer, I., Böhm, R., Jurkovic, A., Lipa, W., Orlik, A., Potzmann, R. et al. (2007) Histalp—historical instrumental climatological surface time series of the Greater Alpine region. *International Journal of Climatology*, 27(1), 17–46.

Ban, N., Caillaud, C., Coppola, E., Pichelli, E., Sobolowski, S., Adinolfi, M. et al. (2021) The first multi-model ensemble of regional climate simulations at kilometer-scale resolution, part I: evaluation of precipitation. *Climate Dynamics*, 57, 275–302.

Beniston, M. (2005) The risks associated with climatic change in mountain regions. In: *Global change and mountain regions*. Dordrecht: Springer, pp. 511–519.

Beniston, M., Diaz, H. & Bradley, R. (1997) Climatic change at high elevation sites: an overview. *Climatic Change*, 36(3), 233–251.

Bigi, A. & Ghermandi, G. (2014) Long-term trend and variability of atmospheric PM_{10} concentration in the Po valley. *Atmospheric Chemistry and Physics*, 14(10), 4895–4907.

Bigi, A., Ghermandi, G. & Harrison, R.M. (2012) Analysis of the air pollution climate at a background site in the Po valley. *Journal of Environmental Monitoring*, 14(2), 552–563.

Brugnara, Y. & Maugeri, M. (2019) Daily precipitation variability in the Southern Alps since the late 19th century. *International Journal of Climatology*, 39(8), 3492–3504.

Ceppi, P., Scherrer, S.C., Fischer, A.M. & Appenzeller, C. (2012) Revisiting Swiss temperature trends 1959–2008. *International Journal of Climatology*, 32(2), 203–213.

Coppola, E., Nogherotto, R., Ciarlo, J.M., Giorgi, F., van Meijgaard, E., Kadygrov, N. et al. (2021) Assessment of the european climate projections as simulated by the large EURO-CORDEX regional and global climate model ensemble. *Journal of Geophysical Research: Atmospheres*, 126(4), e2019JD032356.

Cornes, R.C., van der Schrier, G., van den Besselaar, E.J. & Jones, P.D. (2018) An ensemble version of the E-OBS temperature and precipitation data sets. *Journal of Geophysical Research: Atmospheres*, 123(17), 9391–9409.

Dallan, E., Borga, M., Zaramella, M. & Marra, F. (2021) Enhanced summer convection explains observed trends in extreme subdaily precipitation in the northeastern Italian Alps. *Geophysical Research Letters*, 49(5), e2021GL096727.

Davini, P., Hardenberg, J.V., Corti, S., Christensen, H.M., Juricke, S., Subramanian, A. et al. (2017) Climate SPHINX: evaluating the impact of resolution and stochastic physics parameterisations in the EC-Earth global climate model. *Geoscientific Model Development*, 10(3), 1383–1402.

de Vries, H., Lenderink, G., van der Wiel, K. & van Meijgaard, E. (2022) Quantifying the role of the large-scale circulation on european summer precipitation change. *Climate Dynamics*, 59(9–10), 2871–2886.

Dhital, Y.P., Tang, J., Pokharel, A.K., Tang, Q. & Rai, M. (2022) Impact of aerosol concentration on elevation-dependent warming pattern in the mountains of Nepal. *Atmospheric Science Letters*, 23(10), e1101.

Feser, F., Barcikowska, M., Krueger, O., Schenk, F., Weisse, R. & Xia, L. (2015) Storminess over the North Atlantic and northwestern Europe—a review. *Quarterly Journal of the Royal Meteorological Society*, 141(687), 350–382.

Formetta, G., Marra, F., Dallan, E., Zaramella, M. & Borga, M. (2022) Differential orographic impact on sub-hourly, hourly, and daily extreme precipitation. *Advances in Water Resources*, 159, 104085.

Frei, P., Kotlarski, S., Liniger, M.A. & Schär, C. (2018) Future snowfall in the Alps: projections based on the EURO-CORDEX regional climate models. *Cryosphere*, 12(1), 1–24.

Fuzzi, S., Baltensperger, U., Carslaw, K., Decesari, S., Denier van der Gon, H., Facchini, M.C. et al. (2015) Particulate matter, air quality and climate: lessons learned and future needs. *Atmospheric Chemistry and Physics*, 15(14), 8217–8299.

Giorgi, F. & Coppola, E. (2007) European climate-change oscillation (ECO). *Geophysical Research Letters*, 34(21), L21703.

Giorgi, F., Torma, C., Coppola, E., Ban, N., Schär, C. & Somot, S. (2016) Enhanced summer convective rainfall at alpine high elevations in response to climate warming. *Nature Geoscience*, 9(8), 584–589.

Gobiet, A., Kotlarski, S., Beniston, M., Heinrich, G., Rajczak, J. & Stoffel, M. (2014) 21st century climate change in the European Alps—a review. *Science of the Total Environment*, 493, 1138–1151.

Guariso, G. & Volta, M. (2017) Air quality in Europe: today and tomorrow. In: *Air quality integrated assessment*. Cham: Springer, pp. 1–8.

Haylock, M., Hofstra, N., Klein Tank, A., Klok, E., Jones, P. & New, M. (2008) A European daily high-resolution gridded data set of surface temperature and precipitation for 1950–2006. *Journal of Geophysical Research: Atmospheres*, 113(D20), D20119.

Heinrich, G. & Gobiet, A. (2012) The future of dry and wet spells in Europe: a comprehensive study based on the ensembles regional climate models. *International Journal of Climatology*, 32(13), 1951–1970.

Hersbach, H., Bell, B., Berrisford, P., Hirahara, S., Horányi, A., Muñoz-Sabater, J. et al. (2020) The ERA5 global reanalysis. *Quarterly Journal of the Royal Meteorological Society*, 146(730), 1999–2049.

Hofstra, N., Haylock, M., New, M. & Jones, P.D. (2009) Testing E-OBS European high-resolution gridded data set of daily precipitation and surface temperature. *Journal of Geophysical Research: Atmospheres*, 114(D21), D21101.

Hong, S.-Y., Noh, Y. & Dudhia, J. (2006) A new vertical diffusion package with an explicit treatment of entrainment processes. *Monthly Weather Review*, 134(9), 2318–2341.

Hurrell, J.W. & Deser, C. (2010) North Atlantic climate variability: the role of the North Atlantic oscillation. *Journal of Marine Systems*, 79(3–4), 231–244.

Iacono, M.J., Delamere, J.S., Mlawer, E.J., Shephard, M.W., Clough, S.A. & Collins, W.D. (2008) Radiative forcing by long-lived greenhouse gases: calculations with the aer radiative transfer models. *Journal of Geophysical Research: Atmospheres*, 113(D13), D13103.

Isotta, F.A., Frei, C., Weilguni, V., Perčec Tadić, M., Lassegues, P., Rudolf, B. et al. (2014) The climate of daily precipitation in the Alps: development and analysis of a high-resolution grid dataset from pan-Alpine rain-gauge data. *International Journal of Climatology*, 34(5), 1657–1675.

Jacob, D., Petersen, J., Eggert, B., Alias, A., Christensen, O.B., Bouwer, L.M. et al. (2014) EURO-CORDEX: new high-resolution climate change projections for European impact research. *Regional Environmental Change*, 14(2), 563–578.

Jones, P.W. (1999) First-and second-order conservative remapping schemes for grids in spherical coordinates. *Monthly Weather Review*, 127(9), 2204–2210.

Kahraman, A., Kendon, E.J., Chan, S. & Fowler, H.J. (2021) Quasi-stationary intense rainstorms spread across europe under climate change. *Geophysical Research Letters*, 48, e2020GL092361.

Karl, T.R., Nicholls, N. & Ghazi, A. (1999) Clivar/GCOS/WMO workshop on indices and indicators for climate extremes workshop summary. In: *Weather and climate extremes*. Dordrecht: Springer, pp. 3–7.

Kjellström, E., Nikulin, G., Strandberg, G., Christensen, O.B., Jacob, D., Keuler, K. et al. (2018) European climate change at global mean temperature increases of 1.5 and 2°C above pre-

industrial conditions as simulated by the EURO-CORDEX regional climate models. *Earth System Dynamics*, 9(2), 459–478.

Kotlarski, S., Bosshard, T., Lüthi, D., Pall, P. & Schär, C. (2012) Elevation gradients of European climate change in the regional climate model COSMO-CLM. *Climatic Change*, 112(2), 189–215.

Kotlarski, S., Gobiet, A., Morin, S., Olefs, M., Rajczak, J. & Samacots, R. (2022) 21st century Alpine climate change. *Climate Dynamics*, 60, 65–86.

Kotlarski, S., Keuler, K., Christensen, O.B., Colette, A., Déqué, M., Gobiet, A. et al. (2014) Regional climate modeling on European scales: a joint standard evaluation of the EURO-CORDEX RCM ensemble. *Geoscientific Model Development*, 7(4), 1297–1333.

Kotlarski, S., Lüthi, D. & Schär, C. (2015) The elevation dependency of 21st century European climate change: an RCM ensemble perspective. *International Journal of Climatology*, 35(13), 3902–3920.

Kraaijenbrink, P.D., Bierkens, M., Lutz, A. & Immerzeel, W. (2017) Impact of a global temperature rise of 1.5°C on Asia's glaciers. *Nature*, 549(7671), 257–260.

Kuhn, M. & Olefs, M. (2020) Elevation-dependent climate change in the European Alps. In: *Oxford research encyclopedia of climate science*. Oxford: Oxford Press.

Leutwyler, D., Lüthi, D., Ban, N., Fuhrer, O. & Schär, C. (2017) Evaluation of the convection-resolving climate modeling approach on continental scales. *Journal of Geophysical Research: Atmospheres*, 122(10), 5237–5258.

Matiu, M., Crespi, A., Bertoldi, G., Carmagnola, C.M., Marty, C., Morin, S. et al. (2021) Observed snow depth trends in the European Alps: 1971 to 2019. *Cryosphere*, 15(3), 1343–1382.

Muñoz-Sabater, J., Dutra, E., Agust-Panareda, A., Albergel, C., Arduini, G., Balsamo, G. et al. (2021) ERA5-land: a state-of-the-art global reanalysis dataset for land applications. *Earth System Science Data Discussions*, 13(9), 1–50.

Napoli, A., Crespi, A., Ragone, F., Maugeri, M. & Pasquero, C. (2019) Variability of orographic enhancement of precipitation in the alpine region. *Scientific Reports*, 9(1), 1–8.

Palazzi, E., Filippi, L. & von Hardenberg, J. (2017) Insights into elevation-dependent warming in the Tibetan Plateau-Himalayas from CMIP5 model simulations. *Climate Dynamics*, 48(11), 3991–4008.

Palazzi, E., Mortarini, L., Terzago, S. & Von Hardenberg, J. (2019) Elevation-dependent warming in global climate model simulations at high spatial resolution. *Climate Dynamics*, 52(5), 2685–2702.

Pepin, N., Arnone, E., Gobiet, A., Haslinger, K., Kotlarski, S., Notarnicola, C. et al. (2022) Climate changes and their elevational patterns in the mountains of the world. *Reviews of Geophysics*, 60(1), e2020RG000730.

Pepin, N., Bradley, R.S., Diaz, H., Baraër, M., Caceres, E., Forsythe, N. et al. (2015) Elevation-dependent warming in mountain regions of the world. *Nature Climate Change*, 5(5), 424–430.

Peterson, T., Folland, C., Gruza, G., Hogg, W., Mokssit, A. & Plummer, N. (2001) *Report on the activities of the working group on climate change detection and related rapporteurs*. Geneva: World Meteorological Organization.

Pichelli, E., Coppola, E., Sobolowski, S., Ban, N., Giorgi, F., Stocchi, P. et al. (2021) The first multi-model ensemble of regional climate simulations at kilometer-scale resolution part 2: historical and future simulations of precipitation. *Climate Dynamics*, 56(11), 3581–3602.

Pieri, A.B., von Hardenberg, J., Parodi, A. & Provenzale, A. (2015) Sensitivity of precipitation statistics to resolution, microphysics, and convective parameterization: a case study with the high-resolution WRF climate model over Europe. *Journal of Hydrometeorology*, 16(4), 1857–1872.

Rajczak, J. & Schär, C. (2017) Projections of future precipitation extremes over Europe: a multimodel assessment of climate simulations. *Journal of Geophysical Research: Atmospheres*, 122(20), 10–773.

Rangwala, I. & Miller, J.R. (2012) Climate change in mountains: a review of elevation-dependent warming and its possible causes. *Climatic Change*, 114(3), 527–547.

Rangwala, I., Sinsky, E. & Miller, J.R. (2013) Amplified warming projections for high altitude regions of the Northern Hemisphere mid-latitudes from CMIP5 models. *Environmental Research Letters*, 8(2), 024040.

Rangwala, I., Sinsky, E. & Miller, J.R. (2016) Variability in projected elevation dependent warming in boreal midlatitude winter in CMIP5 climate models and its potential drivers. *Climate Dynamics*, 46(7), 2115–2122.

Russo, S., Sillmann, J. & Fischer, E.M. (2015) Top ten European heatwaves since 1950 and their occurrence in the coming decades. *Environmental Research Letters*, 10(12), 124003.

Rysman, J.-F., Lematre, Y. & Moreau, E. (2016) Spatial and temporal variability of rainfall in the Alps–Mediterranean Euroregion. *Journal of Applied Meteorology and Climatology*, 55(3), 655–671.

Smiatek, G., Kunstmann, H. & Senatore, A. (2016) EURO-CORDEX regional climate model analysis for the Greater Alpine Region: performance and expected future change. *Journal of Geophysical Research: Atmospheres*, 121(13), 7710–7728.

Takayabu, I., Rasmussen, R., Nakakita, E., Prein, A., Kawase, H., Watanabe, S.-I. et al. (2022) Convection-permitting models for climate research. *Bulletin of the American Meteorological Society*, 103(1), E77–E82.

Thompson, G. & Eidhammer, T. (2014) A study of aerosol impacts on clouds and precipitation development in a large winter cyclone. *Journal of the Atmospheric Sciences*, 71(10), 3636–3658.

Tiedtke, M. (1989) A comprehensive mass flux scheme for cumulus parameterization in large-scale models. *Monthly Weather Review*, 117(8), 1779–1800.

Torma, C. & Giorgi, F. (2020) On the evidence of orographical modulation of regional fine scale precipitation change signals: the carpathians. *Atmospheric Science Letters*, 21(6), e967.

Tramblay, Y. & Somot, S. (2018) Future evolution of extreme precipitation in the mediterranean. *Climatic Change*, 151(2), 289–302.

Tudoroiu, M., Eccel, E., Gioli, B., Gianelle, D., Schume, H., Genesio, L. et al. (2016) Negative elevation-dependent warming trend in the eastern Alps. *Environmental Research Letters*, 11(4), 044021.

Valt, M. & Cianfarra, P. (2010) Recent snow cover variability in the Italian Alps. *Cold Regions Science and Technology*, 64(2), 146–157.

Vincent, C., Fischer, A., Mayer, C., Bauder, A., Galos, S.P., Funk, M. et al. (2017) Common climatic signal from glaciers in the European Alps over the last 50 years. *Geophysical Research Letters*, 44(3), 1376–1383.

Viviroli, D., Dürr, H.H., Messerli, B., Meybeck, M. & Weingartner, R. (2007) Mountains of the world, water towers for humanity: typology, mapping, and global significance. *Water Resources Research*, 43(7), W07447.

Xu, J., Grumbine, R.E., Shrestha, A., Eriksson, M., Yang, X., Wang, Y. et al. (2009) The melting Himalayas: cascading effects of climate change on water, biodiversity, and livelihoods. *Conservation Biology*, 23(3), 520–530.

Yao, T., Thompson, L., Yang, W., Yu, W., Gao, Y., Guo, X. et al. (2012) Different glacier status with atmospheric circulations in Tibetan Plateau and surroundings. *Nature Climate Change*, 2(9), 663–667.

Žebre, M., Colucci, R.R., Giorgi, F., Glasser, N.F., Racoviteanu, A.E. & Del Gobbo, C. (2021) 200 years of equilibrium-line altitude variability across the European Alps (1901–2100). *Climate Dynamics*, 56(3), 1183–1201.

Zekollari, H., Huss, M. & Farinotti, D. (2019) Modelling the future evolution of glaciers in the European Alps under the EURO-CORDEX RCM ensemble. *Cryosphere*, 13(4), 1125–1146.

Zubler, E.M., Fischer, A.M., Liniger, M.A., Croci-Maspoli, M., Scherrer, S.C. & Appenzeller, C. (2014) Localized climate change scenarios of mean temperature and precipitation over Switzerland. *Climatic Change*, 125(2), 237–252.

SUPPORTING INFORMATION

Additional supporting information can be found online in the Supporting Information section at the end of this article.

How to cite this article: Napoli, A., Parodi, A., von Hardenberg, J., & Pasquero, C. (2023). Altitudinal dependence of projected changes in occurrence of extreme events in the Great Alpine Region. *International Journal of Climatology*, 1–17. https://doi.org/10.1002/joc.8222